YIC2012 — Universidade de Aveiro
First ECCOMAS Young Investigators Conference
A. Andrade-Campos, N. Lopes, R.A.F. Valente, H. Varum (editors)
24–27 April 2012, Aveiro. Portugal.

Nonlinear modeling of the cyclic response of RC columns

J. Melo [a,*], H. Varum [a], T. Rossetto [b], C. Fernandes [a], A. Costa [a]

[a]UA – University of Aveiro
Department of Civil Engineering
Campus de Santiago
3810-193 Aveiro, Portugal

[b]UCL – University College London
Department of Civil, Environmental & Geomatic Engineering
Gower Street, 101
WC1E 6BT London, UK

**Corresponding author: josemelo@ua.pt*

Abstract. *Cyclic load reversals (like those induced by earthquakes) result in accelerated bond degradation, leading to significant bar slippage. The bond-slip mechanism is reported to be one of the most common causes of damage and even collapse of existing RC structures subjected to earthquake loading. RC structures with plain reinforcing bars, designed and built prior to the enforcement of the modern seismic-oriented design philosophies, are particularly sensitive to bond degradation. However, perfect bond conditions are typically assumed in the numerical analysis of RC structures. This paper describes the numerical modeling of the cyclic response of two RC columns, one built with deformed bars and the other with plain bars and structural detailing similar to that typically adopted in pre-1970s structures. For each column, different modeling strategies to simulate the column response were tested. Models were built using the OpenSees and the SeismoStruct platforms, and calibrated with the available tests results. Within each platform, different types of nonlinear elements were used to represent the columns. Bond-slip effects were included in the OpenSees models resorting to a simple modeling strategy. The models and the parameters adopted are presented and discussed. Comparison is established between the most relevant experimental results and the corresponding results provided by the numerical models. Conclusions are drawn about the capacity of the tested models to simulate the columns response and about the influence of considering or not considering the effects of bars slippage.*

Keywords: non-linear modeling; RC columns; bond-slip mechanism.

1 INTRODUCTION

The hysteretic behavior of reinforced concrete (RC) structures is highly dependent on the interaction between concrete and steel. Cyclic load reversals (like those induced by earthquakes) result in accelerated bond degradation, which leads to significant relative slippage between the reinforcing bars and the surrounding concrete. Plain reinforcing bars, which are present in a large number of existing RC structures that were designed and built before the 1970s, thus prior to the enforcement of the modern seismic-oriented design philosophies, have poor bond properties between concrete and steel. Therefore, RC elements containing this type of steel reinforcement are particularly sensitive to the effects of bar slippage.

The numerical analysis of RC structural elements is usually conducted under the assumption of perfect bond conditions, which may lead to predicted lateral deformation significantly smaller than the real element deformation or to predicted lateral stiffness larger than the existing element stiffness [1]. Bond-slip effects should therefore be included in the numerical models of structural analysis in order to represent more accurately the

elements response [2,3,4,5]. Due to the differences in the interaction mechanisms between concrete and steel in elements with deformed bars (currently used in the RC construction) and elements with plain bars, the models available for simulating the cyclic behavior of RC structural elements with deformed bars are, in general, not adequate for elements with plain bars.

This paper describes the numerical modeling of the cyclic response of two analogous RC columns, one with deformed bars and the other with plain bars and structural detailing similar to that typically found in RC structures designed and built before the 1970s (that is, not adequate for seismic demands). For each column, models were built with the OpenSees and the SeismoStruct platforms, and within each platform different types of beam/column elements were used to represent the column. Particular attention was given to the effects of bar slippage, which were incorporated in the OpenSees models resorting to a simple modeling strategy. The results of the cyclic tests previously conducted on the columns were used to calibrate the adopted models.

After describing the models, comparison is established between the numerical and experimental results in order to conclude about their adequacy to simulate the columns response, and about the importance of including the effects of bar slippage.

2 EXPERIMENTAL PROGRAM AND MATERIAL PROPERTIES

2.1 Column specimens

Figure 1 depicts the geometrical characteristics and reinforcement detailing of the column specimens. Specimen CP was built with plain reinforcing bars and specimen CD was built with deformed bars. The two specimens were built full-scale with the same geometry, dimensions and amount of steel reinforcement. Each specimen consisted of a column with 0.30x0.30m^2 square cross-section and length equal to 2.17m, and of a foundation made by a stiff RC block with 0.30x0.60m^2 cross-section and length equal 1.5m.

Table 1 presents the mean values of the mechanical properties of the concrete and steel reinforcement used in the specimens.

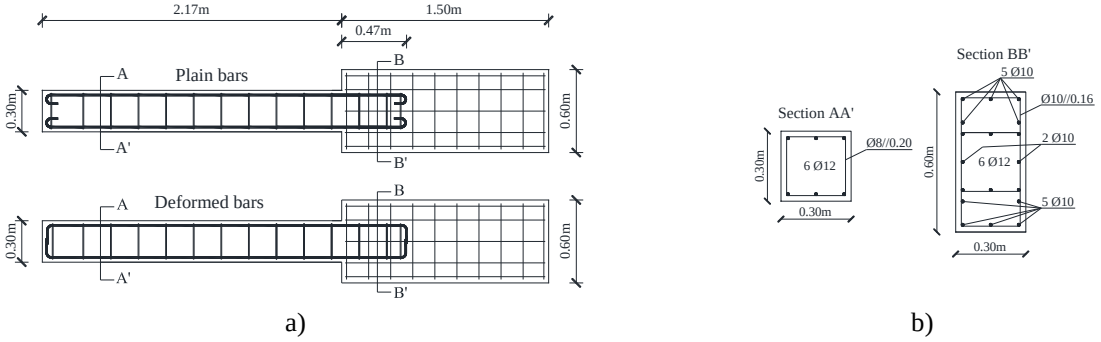

Figure 1: Column specimens: a) dimensions and reinforcement detailing; b) cross-sections.

Table 1: Material mechanical properties (mean values).

Specimen	Type of steel	Concrete		Steel					
				Ø 8 mm			Ø 12 mm		
		(MPa)				(GPa)	(MPa)		(GPa)
		f_{cm}	f_{tcm}	f_{yk}	f_{uk}	E_{ym}	f_{yk}	f_{uk}	E_{ym}
CP	A235 - Plain	17.4	2.1	410	495	198	330	440	199
CD	A400NRSD - Deformed	17.1	2.0	470	605	198	480	610	199

2.2 Test setup and loading conditions

Figure 2 shows the test setup adopted and the imposed loading conditions. The specimens were tested in the horizontal position. Two high load-carrying capacity devices with reduced friction were placed below the column and two concrete blocks were placed below the foundation to carry the elements' self-weight.

The cyclic tests were carried out under displacement-controlled conditions. Two hydraulic actuators were arranged at the columns' top, one to impose the lateral displacements (d_c) and another for the axial force (N). The lateral displacement history is presented in Figure 2-a. The axial force was constant and equal to 305kN.

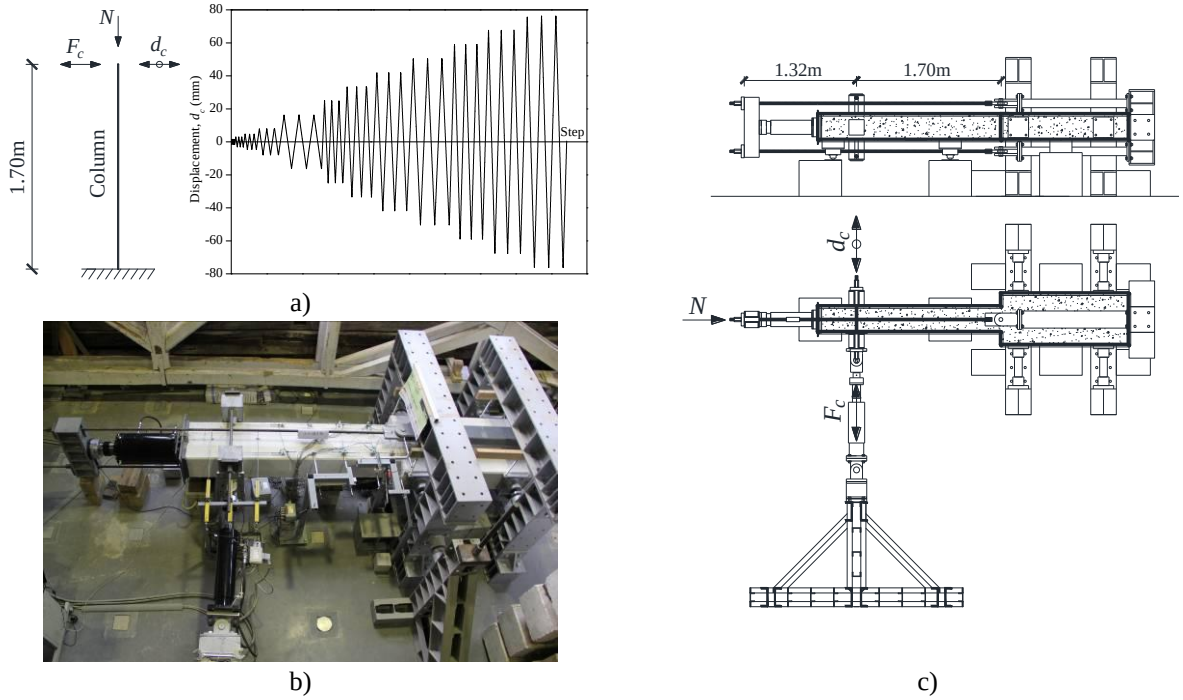

a) b) c)

Figure 2: Test setup: a) support and loading conditions idealized and lateral displacement history; b) general view; c) schematics.

3 NUMERICAL MODELS

3.1 Numerical modeling with OpenSees

The Open System for Earthquake Engineering (OpenSees) is an open source software framework for finite analysis. It was developed to simulate the response of structural and geotechnical systems subjected to earthquakes.

For each column specimen, four nonlinear models were built to simulate the columns response, namely: i) model with *nonlinearBeamColumn element* with distributed plasticity; ii) model with *BeamWithHinges element*, in which the plasticity is considered to be concentrated over specified hinge lengths at the element ends; iii) model with *nonlinearBeamColumn element* and *zero-length section element*; and, iv) model with *BeamWithHinges element* and *zero-length section element*. The *zero-length section element* was incorporated to simulate the effects of the bar slippage associated with the strain penetration and the bond-slip mechanism.

The cross-section of the elements is idealized through fiber modeling. The elements are represented by unidirectional fibers to which are assigned the proper material stress-strain relationships describing the materials monotonic response and hysteretic rules. It should be noted that the columns' foundation was not considered in either of the models under investigation.

3.1.1 *NonlinearBeamColumn element*

The *nonlinearBeamColumn element* is based on the non-iterative (or iterative) force formulation and considers the spread of plasticity along the element. The integration along the element is based on Gauss-Lobatto quadrature rule. The element is prismatic and it is represented by fiber sections at each integration point (see Figure 3). In this study, five integration points were adopted for the column element.

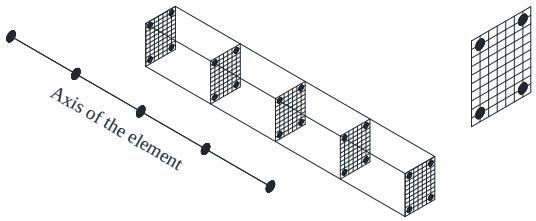

Figure 3: *NonlinearBeamColumn element* with spread of plasticity and five integration points.

3.1.2 *BeamWithHinges element*

The *BeamWithHinges element* is based on the non-iterative (or iterative) flexibility formulation [6]. The element considers plasticity to be concentrated over specified hinge lengths at the elements ends (plastic hinges). This element is divided into three parts: two hinges at the ends and a linear-elastic region in the middle. The Gauss integration points are located in the hinge regions.

In the models under investigation, the length adopted for the plastic hinges correspond to the values measured in the cyclic tests, that is, 0.30m for the column specimen with plain reinforcing bars and 0.35m for the specimen with deformed bars.

3.1.3 *Zero-length section element*

The *zero-length section element* available in OpenSees have a unit-length such that the element deformations are the same that the section deformations. The unit length assumption also implies that the material model for the steel fibers in the *zero-length section element* represents the bar slip instead of strain for a given bar stress. Therefore, a specific material model, defined by a bar stress-slip relationship, should be assigned to the steel fibers of the *zero-length section element*. If placed at the end of a beam/column element, this element can be used to incorporate the fixed-end rotation caused by strain penetration and bond-slip to the beam/column element [6]. A duplicate node (two nodes with the same coordinates) is required to define the *zero-length section element*. Because the shear resistance is not included in the element, the relative translational degree-of-freedom of these nodes should be constrained to each other to prevent sliding of the beam/column element under lateral loads.

In the models under investigation, the *zero-length section element* was placed at the end of the beam/column element (Figure 4), coincident with the node to which were assigned the restraints that simulate the columns' support conditions adopted in the cyclic test.

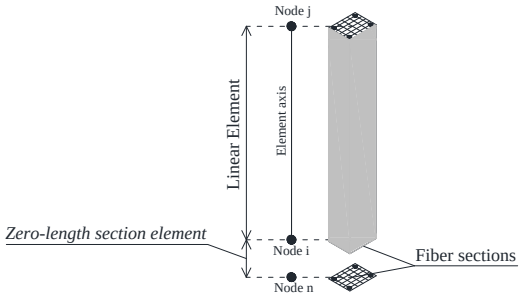

Figure 4: Linear element and *zero-length section element*.

3.1.4 Material models and bar stress-slip model

In the models of the RC columns, the *Concrete02* model and *Steel02* model were adopted for the concrete and steel reinforcement respectively. It should be noted that the elastic part of the *BeamWithHinges element* was modeled using an elastic material with the same elastic modulus of the concrete. The *Concrete02* model was also assigned to the concrete fibers of the *zero-length section element*. The concrete model considers the concrete tensile strength, and takes into account the confinement effect due to the longitudinal bars and the stirrups based on the law proposed by [7] and adapted by [8]. For each column specimen, the values adopted for the *Concrete02*

model parameters were the same in the four models. The adopted values are presented in Table 2, where f_{cm}, f_{cum}, and f_{ctm} are the mean values of compressive strength, residual compressive strength (20% of the maximum compressive strength) and tensile strength respectively. The parameters ε_0, ε_u, and ε_{0t} are the strain corresponding to the compressive, residual and tensile strengths, respectively.

The *Steel02* model is based on the Giuffré-Pinto formulation, implemented later by Menegotto and Pinto [9]. For each column specimen, the values adopted for the *Steel02* model parameters were the same in the four models. The steel mechanical properties are those previously presented in Table 1. The values adopted for the other model parameters are presented in Table 3, where *bst* is the ratio between post-yield tangent and initial elastic tangent, and *R0* is the parameter that controls the transition from elastic to plastic branches.

The bar-stress slip model *Bond_SP01* model available in OpenSees was only assigned to the steel fibers in the *zero-length section element*. This generic model was proposed by Zhao and Sritharan [10] based on the results from pull-out tests of deformed steel reinforcing bars anchored in concrete footings with sufficient embedment length, loaded at the free end zone, specifically on the measured bar stress and loaded end slip evolutions [10]. The values adopted for the model parameters are indicated in Table 3, where α is a tuning parameter used for adjusting the local bond stress-slip relationship, *b* is a stiffness reduction, and *R* is a pinching factor for the cyclic relationship between bar stress and slip. As stated above, the model was calibrated for elements deformed bars. For taking into account the presence of plain bars, parameter α was made equal to 0.5 in the model of specimen CP, as recommended in [11]. For specimen CD, parameter α was made equal to 0.4, as in the model proposed by Zhao and Sritharan [10] and also as recommended in [11]. The slip values corresponding to the yielding strength (S_y) and ultimate strength (S_u) were computed using the equations proposed by Zhao and Sritharan [10].

Table 2: Values adopted for the *Concrete02* model parameters.

Specimen	Concrete	f_{cm} (MPa)	ε_0 (‰)	f_{cum} (MPa)	ε_u (‰)	f_{ctm} (MPa)	ε_{0t} (‰)
CP	Unconfined	17.4	2.1	3.5	10.0	2.0	0.24
	Confined	18.2	2.2	3.6	33.0	2.5	0.30
CD	Unconfined	17.1	2.1	3.4	10.0	2.0	0.24
	Confined	18.1	2.4	3.6	33.0	2.5	0.30

Table 3: Values adopted for the *Steel02* and *Bond_SP01* model parameters.

Material model	Parameter	CP	CD
Steel02	*bst*	0.037	0.044
	R0	12.0	15.5
Bond_SP01	α	0.50	0.40
	b	0.30	0.40
	s_y	0.46 (mm)	0.44 (mm)
	s_u	$40s_y$ (mm)	$40s_y$ (mm)
	R	0.30	0.80

3.2 Numerical modeling with SeismoStruct

The SeismoStruct is a finite element package capable of predicting the large displacements behavior of space frames under static or dynamic loading, taking into account geometric nonlinearities and material inelasticity [12]. Several models are available for concrete and steel materials as well as for the frame elements.

For each column specimen, two nonlinear models were built to simulate the columns response. Similarly to what was adopted for the OpenSees analysis, one model was built with inelastic frame elements with distributed plasticity (*infrmFB element*), whereas another model was built with inelastic plastic hinge frame elements (*infrmFBPH element*) with the nonlinearity concentrated within a fixed length of the element (plastic hinge). Both elements have a force-based formulation and the cross-sections are idealized through fiber modeling. The effects of bar slippage were not incorporated in the SeismoStruct models.

With regard to the material models, the *con_ma* model and the *stl_mp* model available in SeismoStruct were

adopted for the concrete and steel reinforcement respectively.
The *con_ma* concrete model is an uniaxial nonlinear constant confinement model that follows the constitutive relationship proposed by Mander *et al.* [13]. The values adopted for the *Concrete02* model parameters in OpenSees (Table 2) were also adopted for the *con_ma* model parameters.
The *stl_mp* steel model is based on the stress-strain relationship proposed by Menegotto and Pinto [9], coupled with the isotropic hardening rules proposed by Filippou *et al.* [14]. The steel mechanical properties adopted are those previously presented in Table 1. Regarding the other model parameters, the default values indicated by SeismoStruct were adopted, except for R_0, which was made equal to 19.5 instead of 20.0 (default value). This parameter controls the shape of the transition curve between initial and post-yield stiffness.

4 NUMERICAL RESULTS

In this section are presented and discussed the results from the numerical analyses carried out to simulate the cyclic response of the two RC columns. Comparison is established between the numerical and experimental results, namely in terms of force-drift diagrams and energy dissipation. The drift values correspond to the column top displacements divided by the height of the column (1.7m). The dissipated energy is the cumulative sum of the energy dissipation associated with each cycle, corresponding to the area inside the loops in the force-drift diagrams.
It should be noted that the experimental results of specimen CD are presented only up to 3.5% and not 5% (maximum imposed drift) due to problems with the data acquisition system.

4.1 Specimen with plain reinforcing bars (CP)

Figure 5 compares the experimental force-drift diagrams with those obtained from the numerical models under investigation. The software platform used to conduct the numerical analysis, and the type of beam/column element used to represent the column specimen are properly identified.
The SeismoStruct models, with distributed plasticity or concentrated plasticity, provide a relatively better simulation of the column response when compared to the corresponding OpenSees models. A better approximation to the experimental results was attained namely in terms of the maximum strength and ultimate strength (force at maximum drift). The initial stiffness is however relatively better reproduced in the OpenSees models. Within the same software, a better fit to the experimental results was obtained by considering the plasticity concentrated in the plastic hinge regions, instead of distributed along the column length. This was observed to be particularly relevant in the OpenSees models. In particular, the differences in maximum strength and ultimate strength were reduced from 2.7% to 0.5% and from 36.6% to 18.2% respectively. Including the effects of bar slippage in the OpenSees models enhanced the numerical response namely in terms of stiffness of the unloading branches.
The best fit to the experimental results was obtained by the OpenSees model with concentrated plasticity (*BeamWithHinges element*) and considering bar slippage (*zero-length section element*). Conversely, the worst simulation was provided by the OpenSees model with distributed plasticity. However, it should be noted that neither of the models under investigation was able to properly capture the stiffness of the reloading branches, nor the strength degradation, nor the pinching effect.
Figure 6 shows the evolutions of dissipated energy determined from the experimental and numerical results. Table 4 shows the ratio between the experimental and numerical values of cumulative dissipated energy at different values of drift. All the tested models overestimate the experimental values in terms of energy dissipation, namely after 1% drift. The model that led to the best agreement between the numerical and experimental results was also the OpenSees model (OS) with concentrated plasticity *BeamWithHinges elements* and *zero-length section element* (that is, considering the effects of bar slippage). At the maximum drift, the corresponding dissipated energy is 38% higher than the experimental energy. The SeismoStruct model (SS) with distributed plasticity elements conducted to the worst simulation. In this case, the numerical dissipated energy at the maximum drift is about 2 times the experimental energy. Also in accordance with what was previously concluded for the force-drift diagrams, considering the plasticity concentrated in the plastic hinge regions instead of distributed along the column length led to a better reproduction of the dissipated energy evolution. By considering the effects of bar

slippage, the differences in dissipated energy at the maximum drift between the numerical and experimental results are reduced in about 30%.

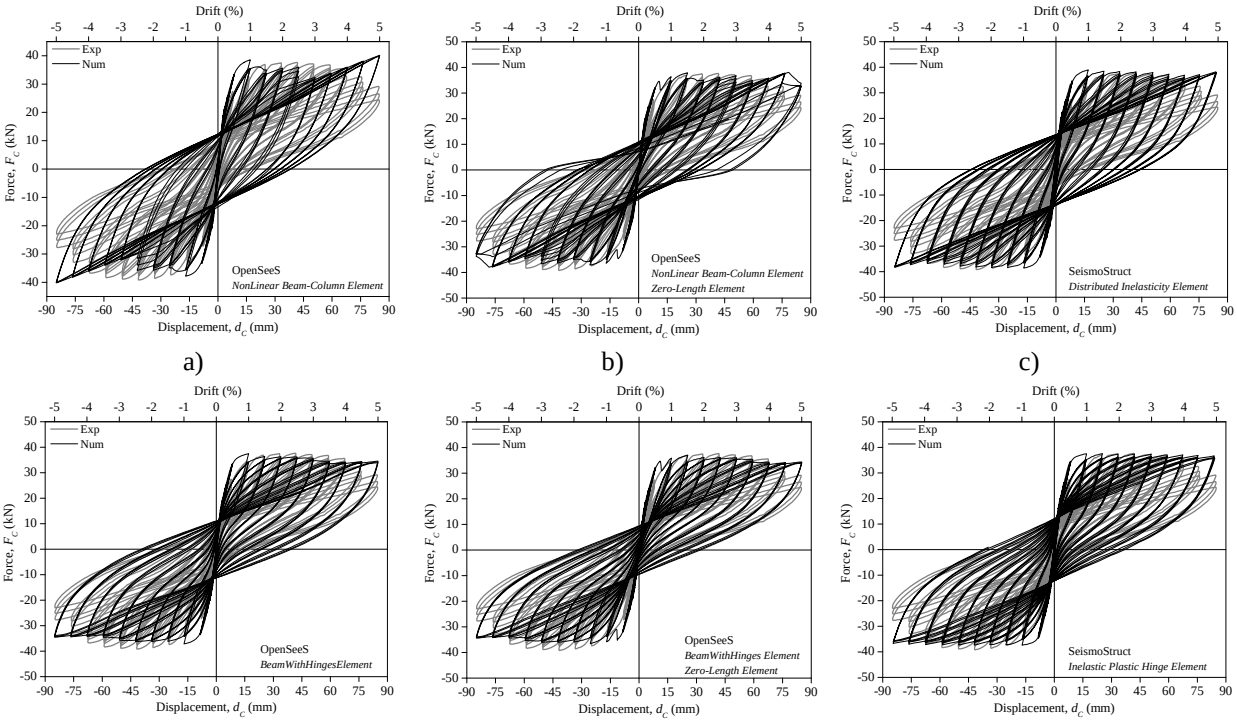

Figure 5: Comparison between the experimental and numerical force-drift diagrams of specimen CP: a), b) and c) numerical results considering elements with distributed plasticity; d), e) and f) numerical results considering elements with plastic hinges.

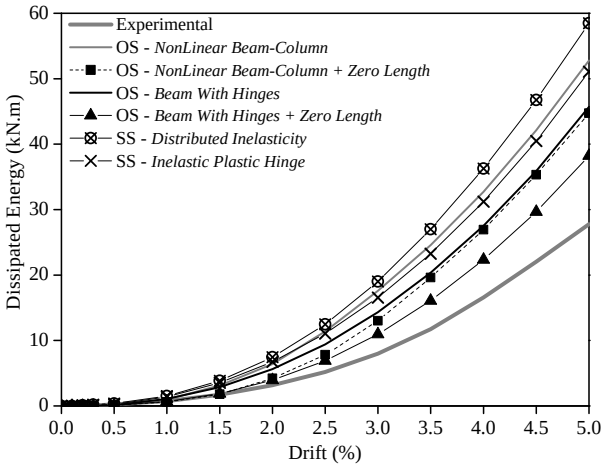

Figure 6: Evolution of dissipated energy for specimen CP.

Table 4: Experimental to numerical dissipated energy ratio for different levels of drift in specimen CP.

Element model	Dissipated energy ratio			
	Drift 1.0%	Drift 2.0%	Drift 3.5%	Drift 5.0%
OS – NonLinear Beam-Column	1.30	2.02	2.09	1.90
OS – NonLinear Beam-Column + Zero Length	0.79	1.32	1.67	1.61
OS – Beam With Hinges	1.43	1.77	1.74	1.65
OS – Beam With Hinges + Zero Length	0.91	1.24	1.37	1.38
SS – Distributed Inelasticity	2.02	2.35	2.30	2.11
SS – Inelastic Plastic Hinge	1.84	2.12	1.98	1.84

4.2 Column specimen with deformed bars (CD)

Figure 7 compares the experimental force-drift diagrams with those obtained from the numerical models under investigation. The software platform used to conduct the numerical analysis, and the type of beam/column element used to represent the column specimen are properly identified.

The differences between the numerical results provided by the SeismoStruct models, with distributed plasticity or concentrated plasticity, and those provided by the corresponding OpenSees models are minor, in terms of both force and stiffness. Similarly to what was concluded for the column specimen with plain reinforcing bars, a better fit to the experimental results of the column specimen with deformed bars was obtained by considering the plasticity concentrated in the plastic hinge regions instead of distributed along the column length. In particular, the stiffness is significantly better reproduced. The initial stiffness is however better simulated in the models with distributed plasticity. Adding the *zero-length section element* in the OpenSees models led to an additional enhancement of the numerical simulation of the force-drift envelope.

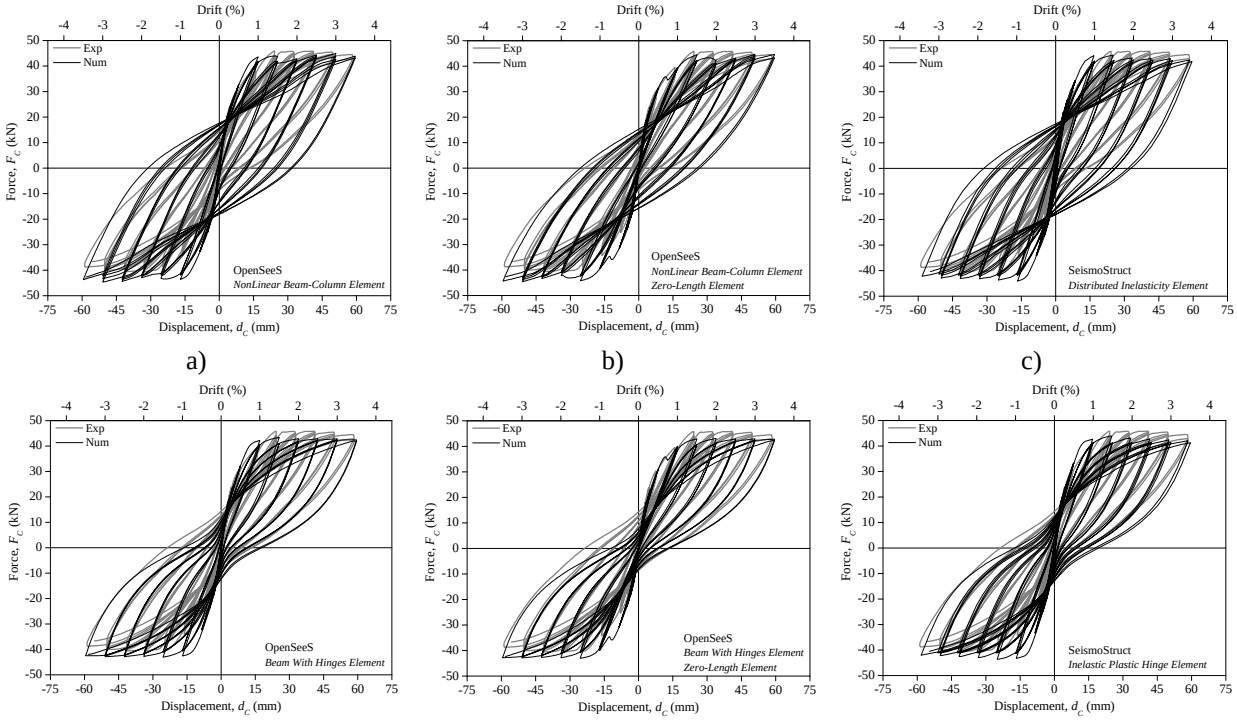

Figure 7: Numerical force-drift diagrams for specimen CD: a), b) and c) considering plasticity distributive elements; d), e) and f) for plastic hinge elements.

As concluded for the column specimen with plain bars, the best fit to the experimental force-drift response (namely to the corresponding peak envelope) was obtained by the OpenSees model with *BeamWithHinges element* and *zero-length section element*. However, the importance of considering the effects of bars slippage in

the numerical modeling of the column specimen with deformed bars is observed to be not as relevant as for the column specimen with plain bars.

Figure 8 depicts the numerical and experimental evolutions of dissipated energy. Table 5 gives the ratio between the experimental and numerical values of cumulative dissipated energy at different values of drift. All the tested models overestimate the experimental values in terms of energy dissipation, namely after 1% drift. The best fit to experimental results was provided by the OpenSees (OS) model with *BeamWithHinges element* and *zero-length section element*. At the maximum drift, the corresponding dissipated energy is 10% higher than the experimental energy. Conversely, the SeismoStruct (SS) model with *Distributed Inelasticity* element conducted to the worst simulation, overestimating in 65% the energy at the maximum drift. By considering the effects of bar slippage, the differences in dissipated energy at the maximum drift between the numerical and experimental results were reduced in 37% and 28% regarding the models with distributed plasticity and concentrated plasticity respectively. For the column specimen with plain bars, the corresponding reductions (at 3.5% drift) are equal to 42% and 37%, therefore showing that considering the effects of bar slippage towards a better simulation of the energy dissipation was relatively more relevant for this specimen. Comparing Table 4 with Table 5 it is shown that the evolution of dissipated energy was generally better reproduced for the column specimen with deformed bars than for the column specimen with plain bars.

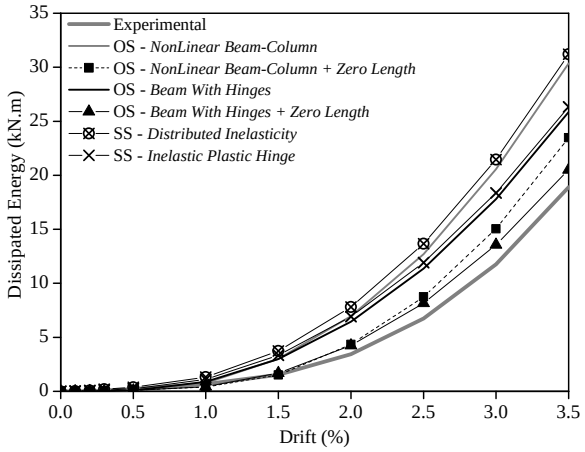

Figure 8: Evolution of the dissipated energy in specimen CD.

Table 5: Experimental and numerical dissipated energy ratio for different levels of drift in specimen CD.

Element model	Dissipated energy ratio		
	Drift 1.0%	Drift 2.0%	Drift 3.5%
OS – NonLinear Beam-Column	1.13	2.02	1.61
OS – NonLinear Beam-Column + Zero Length	0.62	1.25	1.24
OS – Beam With Hinges	1.31	1.86	1.36
OS – Beam With Hinges + Zero Length	0.64	1.23	1.08
SS – Distributed Inelasticity	1.97	2.26	1.65
SS – Inelastic Plastic Hinge	1.64	2.01	1.39

5 FINAL COMMENTS

In this paper was investigated the adequacy of different models to simulate the cyclic behavior of two analogous RC column specimens, one built with plain bars and the other with deformed bars. Models were built with the OpenSees and the SeismoStruct platforms. Within each platform, nonlinear beam/column elements with distributed plasticity or concentrated plasticity were used to represent the columns. The influence of considering the effects of bar slippage in the numerical modeling was also investigated. For each column specimen,

comparison was established between the numerical and experimental results, namely in terms of force-drift diagrams and evolution of dissipated energy. The main conclusions draw for the conducted analyses, are:

i) All the tested models provided a generally satisfactory simulation of the experimental force-drift diagrams. However, neither of the models was able to properly capture the strength degradation, nor the stiffness of the reloading branches, nor the pinching effect (namely in the response of the column specimen with plain bars);
ii) The differences in using OpenSees or SeismoStruct (considering distributed or concentrated plasticity) were minor for the column specimen with deformed bars. Disregarding the effects of bar slippage, a general better fit to the experimental results of the column with plain bars was obtained using OpenSees;
iii) For both the column specimens, a better agreement between the numerical and experimental results (force, stiffness and energy dissipation) was obtained considering the plasticity concentrated in the plastic hinge regions, either in the OpenSees or in the SeismoStruct models. This was particularly relevant for the column specimen with plain bars;
iv) For both the column specimens, the best fit to the experimental results was obtained by incorporating the effects of bar slippage in the OpenSees models with concentrated plasticity. This was particularly relevant for the column specimen with plain reinforcing bars, namely in terms of stiffness and energy dissipation.

Focusing on the bar slippage effects, the results of the analyses presented confirm how important it is to include bond-slip in the numerical modeling of RC structural elements with plain reinforcing bars in order to represent more accurately their cyclic response. However, there is a need for specific models to account for the effects of the bond-slip mechanism in the presence of this type of steel reinforcement.

ACKNOWLEDGEMENT

This paper reports research developed under financial support provided by "FCT - Fundação para a Ciência e Tecnologia", Portugal, namely through the PhD grant of the first author, with reference SFRH/BD/62110/2009.

REFERENCES

[1] Sezen, H.; Setzler, E.J.; Reinforcement Slip in Reinforced Concrete Columns. ACI Structural Journal 105(3):280-289, 2008.
[2] Varum, H.; Seismic assessment, strengthening and repair of existing buildings. PhD Thesis. University of Aveiro. Aveiro. Portugal. 2003.
[3] Kwak, HG.; Improved numerical approach for the bond-slip behavior under cyclic loads, Structural Engineering and Mechanics 5(5):663-677, 1997.
[4] Youssef, M.; Ghobarah, A.; Strength Deterioration due to Bond Slip and Concrete Crushing in Modeling of Reinforced Concrete Members. ACI Structural Journal 96(6):956-966, 1999.
[5] Melo, J.; Fernandes, C.; Varum, H.; Rodrigues, H.; Costa, A.; Arêde, A.; Numerical modelling of the cyclic behaviour of RC elements built with plain reinforcing bars, Engineering Structures, Elsevier, (2):273-286, 2011.
[6] Mazzoni S., McKenna F., Scott M.H., Fenves G.L.; OpenSees Command Language Manual. Pacific Earthquake Engineering Research Center, University of California, Berkeley, U.S.A. 2007.
[7] Hognestad E.; A Study of Combined Bending and Axial Load in Reinforced Concrete. Bulletin Series 339, Univ. of Illinois Exp. Sta., Illinois, U.S.A. 1951.
[8] Guedes JM.; Seismic Behaviour of Reinforced Concrete Bridges. Modelling, Numerical Analysis and Experimental Assessment. PhD Thesis. Faculty of Engineering of the University of Porto, Porto, Portuga. 1997.
[9] Menegotto M.; Pinto P.; Method of analysis for cyclically loaded reinforced concrete plane frames including changes in geometry and non-elastic behaviour of elements under combined normal force and bending. In: IABSE Symposium: Resistance and Ultimate Deformability of Structures Acted on by Well Defined Repeated Loads, Final Report, Lisbon, Portugal. 1973.
[10] Zhao J.; Sritharan S.; Modelling of strain penetration effects in fibre-based analysis of reinforced concrete structures. ACI Structural Journal 104(2):133-141. 2007.
[11] FIB, Task Group 2.5: Bond Models; Bond of Reinforcement in Concrete. State-of-the-art report. FIB Bulletin 10, Lausanne. ISBN 978-2-88394-050-5, 2000.
[12] Seismosoft; Seismostruct, available on the internet site: http://www.seismosoft.com/en/SeismoStruct.aspx, 2012.
[13] Mander J.B.; Priestley M.J.N.; Park R.; Theoretical stress-strain model for confined concrete. Journal of Structural Engineering, 114(8):1804-1826, 1988.
[14] Filippou F.C.; Popov E.P.; Bertero V.V.; Effects of bond deterioration on hysteretic behaviour of reinforced concrete joints. Report EERC 83-19, Earthquake Engineering Research Center, University of California, Berkeley, 1983.